Internet Electronic Journal of Molecular Design **2004**, *3*, 443–463 ISSN 1538–6414
BioChem Press http://www.biochempress.com

Inter*net* Electronic Journal of Molecular Design

August 2004, Volume 3, Number 8, Pages 443–463

Editor: Ovidiu Ivanciuc

Proceedings of the Internet Electronic Conference of Molecular Design, IECMD 2003
November 23 – December 6, 2003
Part 2

A Graphical Similarity Function to Help Ligand Docking to Proteins Based on the Molecular Lipophilicity Potential. The Case of the D_2 Dopamine Receptor

Pierre–Alain Carrupt,[1] Isabelle Raynaud,[1] David McLoughlin,[2] Géraldine Bouchard,[1] Patrick Gaillard,[1] Frédéric Billois,[1] Patrizia Crivori,[1] Philip G. Strange,[2] and Bernard Testa [1]

[1] Institut de Chimie thérapeutique, Section de pharmacie, Université de Lausanne, CH–1015 Lausanne, Switzerland
[2] School of Animal and Microbial Sciences, University of Reading, Whiteknights, Reading, RG6 6AJ, UK

Received: November 19, 2003; Accepted: March 15, 2004; Published: August 31, 2004

Citation of the article:
P.–A. Carrupt, I. Raynaud, D. McLoughlin, G. Bouchard, P. Gaillard, F. Billois, P. Crivori, P. G. Strange, and B. Testa, A Graphical Similarity Function to Help Ligand Docking to Proteins Based on the Molecular Lipophilicity Potential. The Case of the D_2 Dopamine Receptor, *Internet Electron. J. Mol. Des.* **2004**, *3*, 443–463, http://www.biochempress.com.

Internet Electronic Journal of Molecular Design

BioChem Press
http://www.biochempress.com

A Graphical Similarity Function to Help Ligand Docking to Proteins Based on the Molecular Lipophilicity Potential. The Case of the D_2 Dopamine Receptor[#]

Pierre–Alain Carrupt,[1,*] Isabelle Raynaud,[1] David McLoughlin,[2] Géraldine Bouchard,[1] Patrick Gaillard,[1] Frédéric Billois,[1] Patrizia Crivori,[1] Philip G. Strange,[2] and Bernard Testa [1]

[1] Institut de Chimie thérapeutique, Section de pharmacie, Université de Lausanne, CH–1015 Lausanne, Switzerland
[2] School of Animal and Microbial Sciences, University of Reading, Whiteknights, Reading, RG6 6AJ, UK

Received: November 19, 2003; Accepted: March 15, 2004; Published: August 31, 2004

Internet Electron. J. Mol. Des. **2004**, *3* (8), 443–463

Abstract

Motivation. Several recognition forces involved in ligand–receptor binding are also expressed in lipophilicity. Based on the molecular lipophilicity potential (MLP), a graphical tool for visual help in the docking procedure was developed and tested with the docking of dopamine agonists in a model of trans–membrane domain of the D_2 dopamine receptor built by homology.

Method. The MLP similarity function used in this study was built using two Molecular Lipophilicity Potential calculated on the ligand molecular surface, namely the intrinsic MLP (*i.e.* the MLP of the ligand) and the perceived MLP (*i.e.* the MLP generated by the binding site, and hence perceived by the ligand).

Results. The MLP similarity function tool allows to rank the low–energy conformers of a ligand–protein complex, thus affording a criterion to select high–probability binding modes. Interestingly the procedure was also able to correctly predict enantioselectivity.

Conclusions. The MLP similarity score presented here is a graphical tool able to analyze recognition forces between a ligand and a binding site. This method also allows an explanation of the difference in affinity of D_2 receptor between two enantiomers of a ligand and between two structurally related compounds.

Keywords. Molecular lipophilicity potential; molecular recognition; receptor docking; D_2 receptor; dopamine; score function.

[#] Presented in part at the Internet Electronic Conference of Molecular Design, IECMD 2003.

* Correspondence author; E–mail: Pierre–Alain.Carrupt@pharm.unige.ch.

1 INTRODUCTION [1]

The binding constants and biological responses (*e.g.* agonists versus antagonists) of receptor ligands depend largely on their affinity, selectivity and binding modes. These phenomena are governed by intermolecular forces of recognition expressed in the stereoelectronic and stereodynamic match between binding sites and ligands. An assessment of recognition forces is therefore a critical step in understanding and predicting affinity and selectivity.

Lipophilicity is a molecular property that encodes in a single number (*e.g.* the partition coefficient log P) a wealth of information on intramolecular interactions and intermolecular forces [2,3]. In particular, many of the recognition forces involved in ligand–receptor binding contribute to lipophilicity. The molecular lipophilicity potential (MLP) has been developed as a field expressing in three–dimensions and in a conformation–dependent manner the intermolecular forces encoded in lipophilicity [4,5]. As demonstrated in various studies, the MLP can be introduced as an additional field in three–dimensional QSAR (3D–QSAR) computations, leading to successful predictions of binding constants and biological activities [6–10]. This is the indirect approach to defining the stereoelectronic features of a binding site.

In this study, the MLP has been extended and developed into a tool to visualize the stereoelectronic match between ligand and receptor. To this end, two molecular lipophilicity potentials were defined, the intrinsic MLP (*i.e.* the MLP of the ligand on its molecular surface) and the perceived MLP (*i.e.* the MLP generated by the binding site and computed on the ligand molecular surface, and hence perceived by the ligand). Such an approach is only possible when the complete geometry of a binding site is known from X–ray crystallography or has been deduced by homology modeling. Given the nature of the MLP, it is hypothesized that the greater the stability of a ligand–receptor complex, the larger the similarity between the intrinsic and perceived MLPs. To quantify this similarity, we define here a *similarity score* which proves able to discriminate between several binding modes of D_2 dopamine receptor agonists proposed by standard molecular modeling tools. The results indicate that little information was lost in the successive computational steps that led from (*a*) homology modeling of the D_2 dopamine receptor, to (*b*) agonist docking, to (*c*) calculation of ligand and receptor MLPs, and to (*d*) similarity scores of intrinsic and perceived MLPs.

2 MATERIALS AND METHODS

Calculations were performed on Silicon Graphics Indy R4400 175 MHz, O_2 R5000 180 MHz and Origin 2000 4 CPU R10000 195 MHz workstations with hardware stereographics visualization capacities.

2.1 Experimental and Theoretical Support

Direct and circumstantial evidence from site–directed specific mutagenesis studies shows that an important factor in the interaction of ligands with the D_2 dopamine receptor is an electrostatic attraction between Asp114 in the third transmembrane helix (TM III) and the cationic group found in all ligands [11,12]. For an agonist containing a catechol moiety, hydrogen bond interactions with two or three serine residues (Ser193, Ser194, Ser197) contribute to the free energy of binding [13,14]. Hydrophobic residues within the receptor core appear to be crucial for ligand binding to Phe389 and Phe390 in TM VI in the D_2 receptor [15]. Experimental evidence on the mechanism of binding of ligands to the dopamine receptor has been reviewed by Strange [16].

2.2 Computer Software

The model of the D_2 dopamine receptor was based on a refined template of a β_2 adrenergic receptor [17]. This model of the β_2 adrenergic receptor was initially based on the electron microscopy derived coordinates of the α–helices of bacteriorhodopsin but the helices were arranged to agree with data for sensory rhodopsin [17]. The β_2 adrenergic receptor template was installed as Protein Data Bank coordinates into the Polygen Quanta program. The predicted transmembrane domains of the D_2 dopamine receptor were superimposed on their positional equivalents in the β_2 adrenergic receptor template structure using Align and Superpose sub–programs of the Quanta package. Before superimposing the D_2 receptor sequence, helix VII of the β_2 adrenergic receptor was remodeled to remove the bend by using the corresponding helix from bacteriorhodopsin. The model was then energy–minimized with constrained α–helical positions using the Sybyl software.

The strategy to build a homology model of the D_2 receptor raises a number of questions, especially concerning the choice of template (bacteriorhodopsin *vs* rhodopsin), given the recently published structure of bovine rhodopsin [18]. However, no homology model can give the final answer and the older model we used was a test of the methodology presented here mainly due to its globally good agreement with mutagenesis results (see above).

2.3 Docking Procedure

All docking computations were carried out using the SYBYL 6.5 package [19] and the Tripos 5.2 force field [20] including the electrostatic term calculated with Gasteiger–Marsili partial atomic charges [21]. Derivative technique was Conjugate gradient [22] after 200 iterations of the simplex algorithm [23], with a distance–dependent dielectric constant of $\varepsilon = 4.0$ and a non–bonded cut–off of 8.0 Å. This method was chosen because it had sufficient convergence properties.

Binding modes for each ligand–receptor complex were computed using molecular dynamics and energy minimization procedures as summarized in Scheme 1.

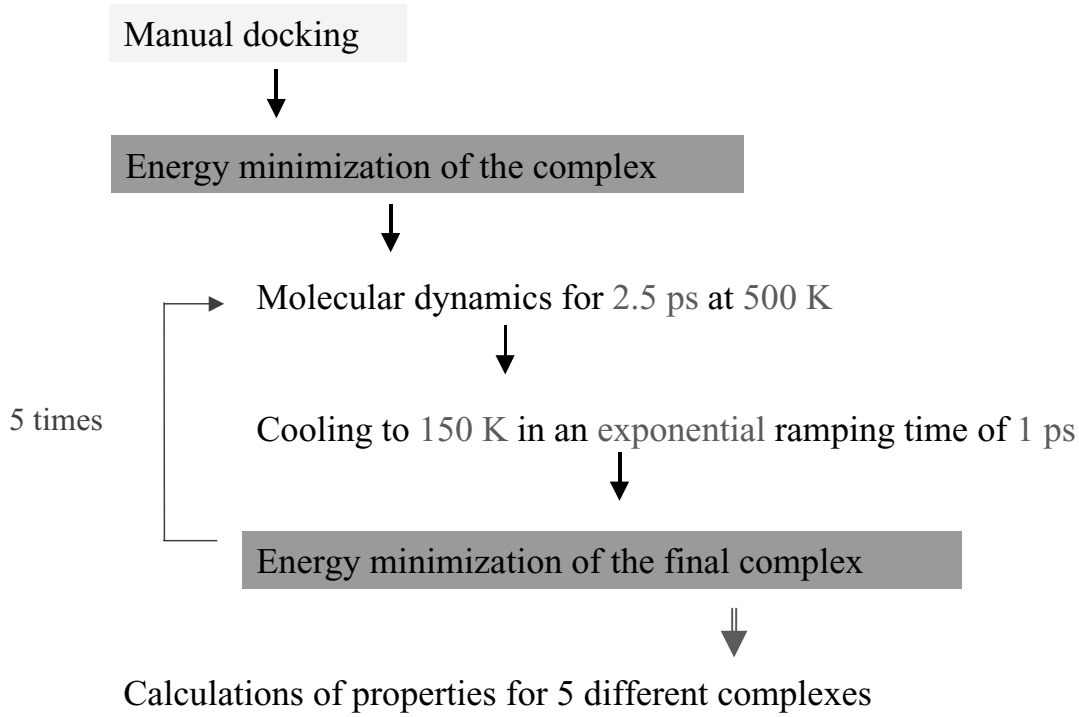

Scheme 1

Primary manual docking of the D_2 ligands shown in Figure 1 were carried out using the command DOCK (SYBYL command). DOCK gives a real–time approximation of interaction energy allowing interactive work. All ligands were docked in their lowest energy conformation determined by high–temperature quenched molecular dynamics [24]. Subsequently, manual modifications of the conformations were performed to better adapt ligands docked into the cavity. The achievement of the manual docking was done in three steps:

1. The main anchor point is the Asp114 in the third transmembrane helix (TM III).
2. The orientation of the ligand is, for steric reasons, perpendicular to the membrane plane to adjust within the binding pocket. This observation has been reported previously [25].
3. Adjustment of the position to allow H–bonding between hydroxyl groups of the ligands and the three serines located in TM V.

Various side–chain conformations were altered manually in order to optimize inter–residue interactions and interactions between side–chains and ligands.

The D_2 receptor model consisted of the TM bundle without the connecting loops. The minor role of the intracellular and extracellular loops in determining ligand recognition in some G–protein coupled receptors (GPCR) has been demonstrated for the β–adrenergic receptor [26–29]. This simplification obviates the difficulty in simulating the behavior of the protein. In order to avoid the destruction of the model during high–temperature dynamics, Cα of TM domains within 4 Å of the ligand, plus all the amino acids beyond 4 Å, were considered as an aggregate. These residues defined a rigid shell around the binding pocket. Thus, only side–chains within 4 Å from the ligand were involved during the dynamics and minimization described below.

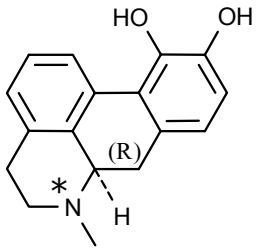

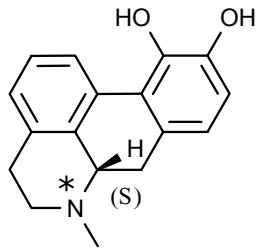

(R)-(-)- and (S)-(+)-Apomorphine

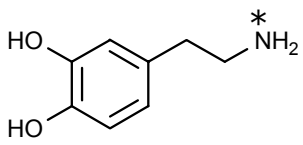

Dopamine

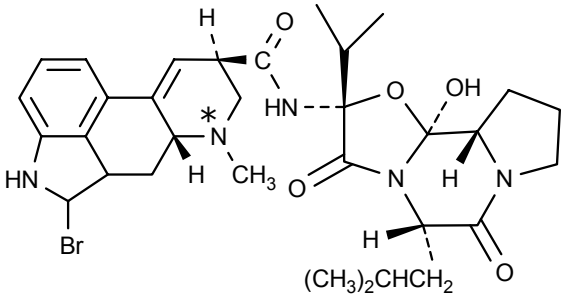

Bromocriptine

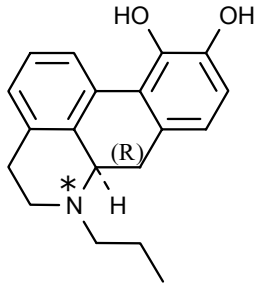

(R)-(-)-Propylnorapomorphine

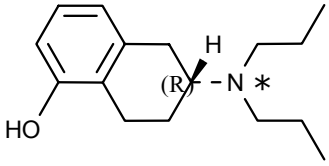

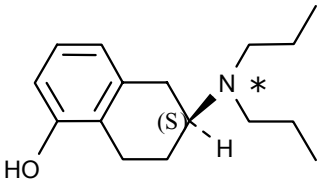

(R)-(+)- and (S)-(-)-5-hydroxy-N,N-di-n-propyl-2-aminotetralin (S-OH-DPAT)

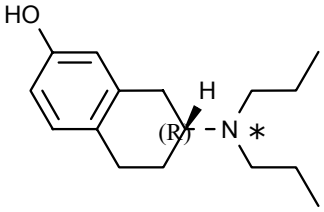

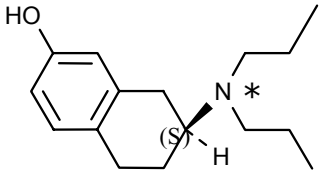

(R)-(+)- and (S)-(-)-7-hydroxy-N,N-di-n-propyl-2-aminotetralin (7-OH-DPAT)

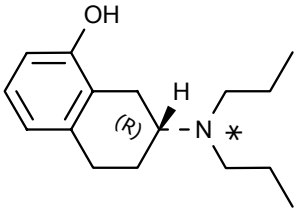

(R)-(+)-8-hydroxy-N,N-di-n-propyl-2-aminotetralin (8-OH-DPAT)

Figure 1. Ligands investigated. Protonation sites used to establish the ionic bond with Asp114 are indicated by an asterisk.

In addition, a harmonic penalty function between the center of mass of the carboxylate moiety of Asp114 and the proton of the ammonium moiety of ligands was used according to site–specific mutagenesis data (see above). This harmonic function was taken as null as long as the distance remained between 0.8 Å and 2.8 Å, and increased by a power of two outside this range. The penalty constant for deviation from the target range was 200 kcal•mol^{-1}•Å^{-2}. This range was chosen based on the atomic surroundings of selected functional groups in ligand–receptor structures recorded in the Brookhaven Protein Databank [30].

Each of the starting complexes so obtained was submitted to a two–step minimization using 200 simplex and Conjugate Gradient iterations until the RMS convergence reached 0.05 kcal•mol^{-1}•Å^{-1}. The resultant structures constituted the starting point for 5 cycles of simulated annealing [31]. A simulated annealing cycle consisted of heating to a temperature of 500 K during a plateau time of 2.5 ps, followed by a decrease to 150 K in an exponential ramping time of 1 ps. Molecular dynamics simulations in such experiments were carried out using the following conditions: the step size was 1 fs; the non–bonded pair list update frequency contained 25 steps; coordinate sets were saved at 50 fs intervals; cut–off distance for non–bonded interactions and dielectric constant were the same as described above for preliminary optimizations. Finally, another two–step minimization was performed on the five cooled complexes followed by MLP similarity calculations for each of the ten agonists. In these final geometry minimizations, the penalty function between the ligand and Asp114 was removed.

Two criteria were used to select the complex with the best match between the ligand and the receptor among the five obtained from the molecular dynamic simulations.

1. The carboxylate moiety of the Asp114 and the proton of the ammonium moiety of the ligand had to be in the range 1.4 Å–2.8 Å. Except for four binding modes of (R)–(–)–apomorphine all the complexes in Table 1 respect the distance range constraint.

2. The preferred binding mode was selected as the one with the highest similarity score.

Secondary headings are numbered, font size 14, centered, bold, and with the first letter of each main word capitalized.

It must be noted that in all retained docking solutions, important variations of ligand conformation and binding pocket geometry (especially for the location of Ser193, Ser194 and Ser197) resulted from molecular dynamics and geometry optimization. Due to the various assumptions made during the stepwise process, the proposed binding modes remain hypothetical even if globally compatible with existing site–directed mutagenesis data. Nevertheless they can be useful guidelines for future more focused mutagenesis experiments.

2.4 MLP and MLP Similarity Scores

The MLP [6] is based on the atomic fragmental system of lipophilicity proposed by Broto *et al*. [32] and on a distance function that defines how the MLP decreases with increasing distance from the molecular surface. Thus, the MLP can be expressed by the general Eq. (1):

$$MLP_k = \sum_{i=1}^{N_{at}} f_i \bullet fct(d_{ik}) \quad (1)$$

where k = label of a given point in space, i = label of the atomic fragment, N = total number of fragments in the molecule, f_i = lipophilic constant of atomic fragment i, fct = distance function, d_{ik} = distance between fragment i and space point k.

With a Fermi distance function [5], Eq. (1) becomes:

$$MLP = \sum_{i=1}^{N_{at}} f_i \bullet \frac{1 + e^{-ab}}{1 + e^{a(d_{ik} - b)}} \quad (2)$$

The molecular surface S+ was generated with the standard software SYBYL using the atomic radii of Gavezzotti [33] increased by 0.3 Å. Different combinations of a and b parameters for 6 different complexes for each ligand were tested. The best result for the score function based on its resolution and its graphical representation were obtained for a = 1.5 and b = 2.5.

The basic assumption in the calculation of the MLP is that the atomic fragmental values represent the added contributions of many intermolecular forces obtained experimentally. The importance of hydrophobic interactions and dispersion forces (which yield positive values in the MLP) is well recognized in homology modeling of proteins and docking experiments of ligands [34,35]. The same is true of polar interactions, in particular H–bonds and electrostatic forces, which yield negative values in the MLP [3,30].

The intrinsic MLP was calculated on the molecular surface S^+ (represented by dots) using the atoms of the ligand and their lipophilic contribution. On the same surface S^+, the perceived MLP was calculated using the atoms of the entire binding site and their lipophilic contribution. The MLP similarity score at each dot of the surface S^+ was computed as the product of perceived and intrinsic MLP. For the whole molecular surface S^+ of the ligand, the similarity score function was computed using Eq. (3):

$$Similarity = \sum_{k=1}^{n_{dots}} MLP_k^{Int} \bullet MLP_k^{Per} \quad (3)$$

where k = index of a given point in space, n_{dots} =total number of dots on the surface S^+, MLP^{Int} = intrinsic MLP, MLP^{Per} = perceived MLP.

When the MLP^{Int} and the MLP^{Per} are of a similar nature and hence have identical sign, their product on a given dot of the ligand surface will be positive, implying a good correspondence

between the two MLPs. In contrast, a negative product characterizes regions of poor correspondence. Eq. (3) should offer a simple and adequate assessment of the similarity between the two MLPs. The MLP similarity score between ligand and receptor was color–coded on the molecular surface of the ligand using a scale ranking from the most different to the most similar regions, namely red, yellow, white, green, green–blue, blue. The color of a dot was set to invisible when no or little interaction existed (*e.g.* a region of the ligand pointing outside the binding pocket).

2.2 Dissociation Constants for Agonists

The dissociation constants of the agonists (Table 1) were obtained from competition studies versus [^{3}H]spiperone and are mostly for D_2 receptors expressed in CHO cells and assayed in the presence of GTP (100 μM) to eliminate coupling between receptor and G–protein.

Table 1. Dissociation constants (pK_i) of agonists for the D_2 dopamine receptor agonists

Compounds	pK_i
Bromocriptine	8.01 [b]
NPA [a]	7.73 [b]
Dopamine	4.86 [c]
(R)–(–)–Apomorphine	6.53 [d]
(S)–(+)–Apomorphine	6.26
(R)–(+)–5–OH–DPAT [e]	5.88 [c]
(S)–(–)–5–OH–DPAT [e]	6.62 [c]
(R)–(+)–7–OH–DPAT [e]	6.41 [c]
(S)–(–)–7–OH–DPAT [e]	4.74 [b]
R)–(+)–8–OH–DPAT [e]	5.30 [c]

[a] (R)–(–)–propylnorapomorphine
[b] Values from ref [56]
[c] Payne and Strange, unpublished data
[d] Values from ref [57]
[e] OH–DPAT = hydroxy–N,N–di–*n*–propyl–2–aminotetralin

3 RESULTS AND DISCUSSION

Table 2 contains the results that allowed us to identify the best binding mode for each ligand, namely the binding mode affording the highest score. A simple visual analysis of the selected binding mode with MLP scores displayed on the molecular surface S^+ is presented in Figures 2 to 7.

3.1 (R)–(+)– and (S)–(–)–7–OH–DPAT

As can be seen in Figure 2, aromatic–aromatic interactions occur with Phe389 for the (R)–(+)–enantiomer of 7–OH–DPAT. There is a wide and intense electrostatic interaction between the Asp114 side–chain and the protonated amino group of the ligand. Hydrophobic interactions can also be seen between Ile397 and Val111 and the *n*–propyl group of (R)–(+)–7–OH–DPAT. Noteworthy is a slightly unfavorable interaction with Ser193 which is too close to the aromatic part of the ligand.

Table 2. Results of simulating annealing and similarity calculations. The selected ligand–receptor conformers are presented in bold.

Complexes [a]	I_e [b]	Score [+ c]	Score [– d]	Score
(R)–(+)–8–OH–DPAT_0	–45.97	1474.5	–290.5	1184.0
(R)–(+)–8–OH–DPAT_1	–50.77	1432.5	–306.5	1126.1
(R)–(+)–8–OH–DPAT_2	–49.65	1469.9	–310.4	1159.4
(R)–(+)–8–OH–DPAT_3	**–48.75**	**1545.0**	**–294.6**	**1250.4**
(R)–(+)–8–OH–DPAT_4	–48.07	1423.2	–355.8	1067.4
(R)–(+)–8–OH–DPAT_5	–48.43	1306.9	–341.6	965.2
Dopamine_0	–32.99	2242.9	–107.6	2135.3
Dopamine_1	**–35.85**	**2466.2**	**–51.2**	**2415.0**
Dopamine_2	–32.48	1655.8	–52.7	1603.0
Dopamine_3	–34.84	1970.7	–141.6	1829.2
Dopamine_4	–32.30	1591.0	–108.8	1482.2
Dopamine_5	–33.56	1998.7	–87.6	1911.1
NPA_0	–41.64	1708.7	–152.3	1556.4
NPA_1	**–45.90**	**1801.5**	**–138.2**	**1663.3**
NPA_2	–45.64	1504.7	–217.7	1287.0
NPA_3	–44.71	1664.9	–206.2	1458.6
NPA_4	–42.69	1381.3	–234.9	1164.4
NPA_5	–47.38	1659.0	–170.0	1489.0
(R)–(+)–7–OH–DPAT_0	–42.80	1548.7	–155.9	1392.8
(R)–(+)–7–OH–DPAT_1	–40.45	1321.3	–148.0	1173.3
(R)–(+)–7–OH–DPAT_2	–43.51	1856.2	–152.9	1703.0
(R)–(+)–7–OH–DPAT_3	–48.73	1664.9	–206.2	1458.6
(R)–(+)–7–OH–DPAT_4	**–43.64**	**1911.4**	**–173.0**	**1738.4**
(R)–(+)–7–OH–DPAT_5	–44.41	1820.3	–230.5	1589.9
(R)–(–)–Apomorphine_0	**–40.69**	**985.1**	**–204.4**	**780.7**
(R)–(–)–Apomorphine_1	–37.39	520.6	–247.6	273.0
(R)–(–)–Apomorphine_2	–37.39	520.6	–247.6	273.0
(R)–(–)–Apomorphine_3	–41.69	910.6	–252.4	658.2
(R)–(–)–Apomorphine_4	–29.12	234.6	–183.5	51.1
(R)–(–)–Apomorphine_5	–33.85	290.0	–327.6	–37.6
(S)–(–)–7–OH–DPAT_0	–42.29	1485.1	–229.4	1255.6
(S)–(–)–7–OH–DPAT_1	–44.54	1376.7	–212.5	1164.2
(S)–(–)–7–OH–DPAT_2	–46.20	1806.0	–160.8	1645.2
(S)–(–)–7–OH–DPAT_3	–42.15	1499.4	–257.8	1241.6
(S)–(–)–7–OH–DPAT_4	**–43.96**	**2142.0**	**–105.7**	**2036.3**
(S)–(–)–7–OH–DPAT_5	–44.90	1851.1	–189.1	1662.0
(R)–(+)–5–OH–DPAT_0	–42.02	1598.6	–174.3	1424.3
(R)–(+)–5–OH–DPAT_1	–44.88	1633.7	–306.9	1326.8
(R)–(+)–5–OH–DPAT_2	–44.91	1796.6	–285.3	1511.3
(R)–(+)–5–OH–DPAT_3	–47.51	1676.7	–287.1	1389.5
(R)–(+)–5–OH–DPAT_4	**–45.58**	**1735.2**	**–194.9**	**1540.3**
(R)–(+)–5–OH–DPAT_5	–44.55	1445.2	–234.9	1210.4
(S)–(–)–5–OH–DPAT_0	–40.79	1490.3	–257.4	1233.0
(S)–(–)–5–OH–DPAT_1	–45.00	1632.3	–123.2	1509.1
(S)–(–)–5–OH–DPAT_2	–45.16	1538.4	–209.3	1329.0
(S)–(–)–5–OH–DPAT_3	**–44.95**	**1881.3**	**–171.8**	**1709.5**
(S)–(–)–5–OH–DPAT_4	–42.75	1806.2	–199.1	1607.1
(S)–(–)–5–OH–DPAT_5	–46.13	1856.6	–219.2	1637.4
(S)–(–)–Apomorphine_0	–39.05	1211.2	–520.6	690.5
(S)–(–)–Apomorphine_1	–40.13	952.3	–515.2	437.2
(S)–(–)–Apomorphine_2	–42.10	1237.6	–397.0	840.6
(S)–(–)–Apomorphine_3	**–42.22**	**1159.6**	**–278.5**	**881.1**
(S)–(–)–Apomorphine_4	–39.16	1021.3	–512.7	508.5
(S)–(–)–Apomorphine_5	–40.13	926.6	–493.3	436.3

Table 2. (Continued)

Complexes [a]	I_e [b]	Score [+ c]	Score [– d]	Score
Bromocriptine1_0	–60.85	1553.0	–906.7	646.3
Bromocriptine1_1	–63.78	1549.2	–801.7	747.5
Bromocriptine1_2	**–60.90**	**1374.6**	**–560.4**	**814.2**
Bromocriptine1_3	–65.03	1439.0	–779.6	659.4
Bromocriptine1_4	–61.51	1173.5	–690.5	483.0
Bromocriptine1_5	–63.49	1220.8	–910.4	310.4
Bromocriptine2_0	–48.45	2523.4	–619.5	1903.8
Bromocriptine2_1	**–75.77**	**2492.8**	**–532.2**	**1960.6**
Bromocriptine2_2	–79.33	2423.1	–566.5	1856.6
Bromocriptine2_3	–76.69	2135.6	–645.4	1490.3
Bromocriptine2_4	–77.69	2254.5	–634.9	1619.6
Bromocriptine2_5	–80.29	2247.8	–697.5	1550.3

[a] Conformers of complexes obtained after the molecular dynamics simulation ranked by interaction energy. The subscript 0 correspond to the geometry of the complex at the beginning of simulated annealing
[b] Interaction energy: difference of energy (in kcal/mol) between the energy of the complex and the sum of the energies of the ligand and receptor
[c] Similarly score calculated from MLPintrinsic and MLPperceived
[d] Dissimilarly score calculated from MLPintrinsic and MLPperceived

For the (S)–(–)–enantiomer, stacking is observed between Phe390 and the cyclohexyl ring. Hydrophobic interactions are seen between Val190 and the rings and between Phe110 and Ile397 and the n–propyl group. Highly unfavorable interactions exist between Ser193 and Ser194 and the ligand. They are revealed by the MLP similarity score which exhibits in this region a large white pocket. Interactions of the three serine residues (Ser193, Ser194 and Ser197) with the catechol moieties of the ligand are critical for ligand binding to the D_2 receptor [13,14]. The two enantiomers can form a H–bond between the hydroxyl group of the ligand and Ser197. However, according to the score functions, the lower affinity of (S)–(–)–7–OH–DPAT for the D_2 receptor can be explained by the very unfavorable interactions with Ser193 and Ser194.

3.2 (R)–(–)– and (S)–(+)–Apomorphine

(R)–(–)–Apomorphine also exhibits π–stacking interactions with Phe389 and Phe390. Hydrophobic interactions between Val190 and the ligand are also observed as well as a broad unfavorable region due to interactions of the polar Ser193 with the hydrophobic region of the molecule. (S)–(+)–Apomorphine presents a different pattern of interactions. The interactions with Phe389 and Phe390 are weaker and due to orthogonal aromatic–aromatic interactions more than to genuine stacking. There are favorable interactions between His393, Asn418 and the ligand, but there is also a highly unfavorable region due to interaction of the polar Cys118 with the hydrophobic region of the molecule. This pattern explains the lower affinity of the (S)–(+)–enantiomer. (R)–(–)–Apomorphine is able to form H–bonds with Ser193 and Ser194, but not with Ser197. In contrast, its (S)–(+)–enantiomer is able to form an H–bond only with Ser193. The reduced ability to make these bonds may explain the lower affinity of the (S)–(+)–enantiomer.

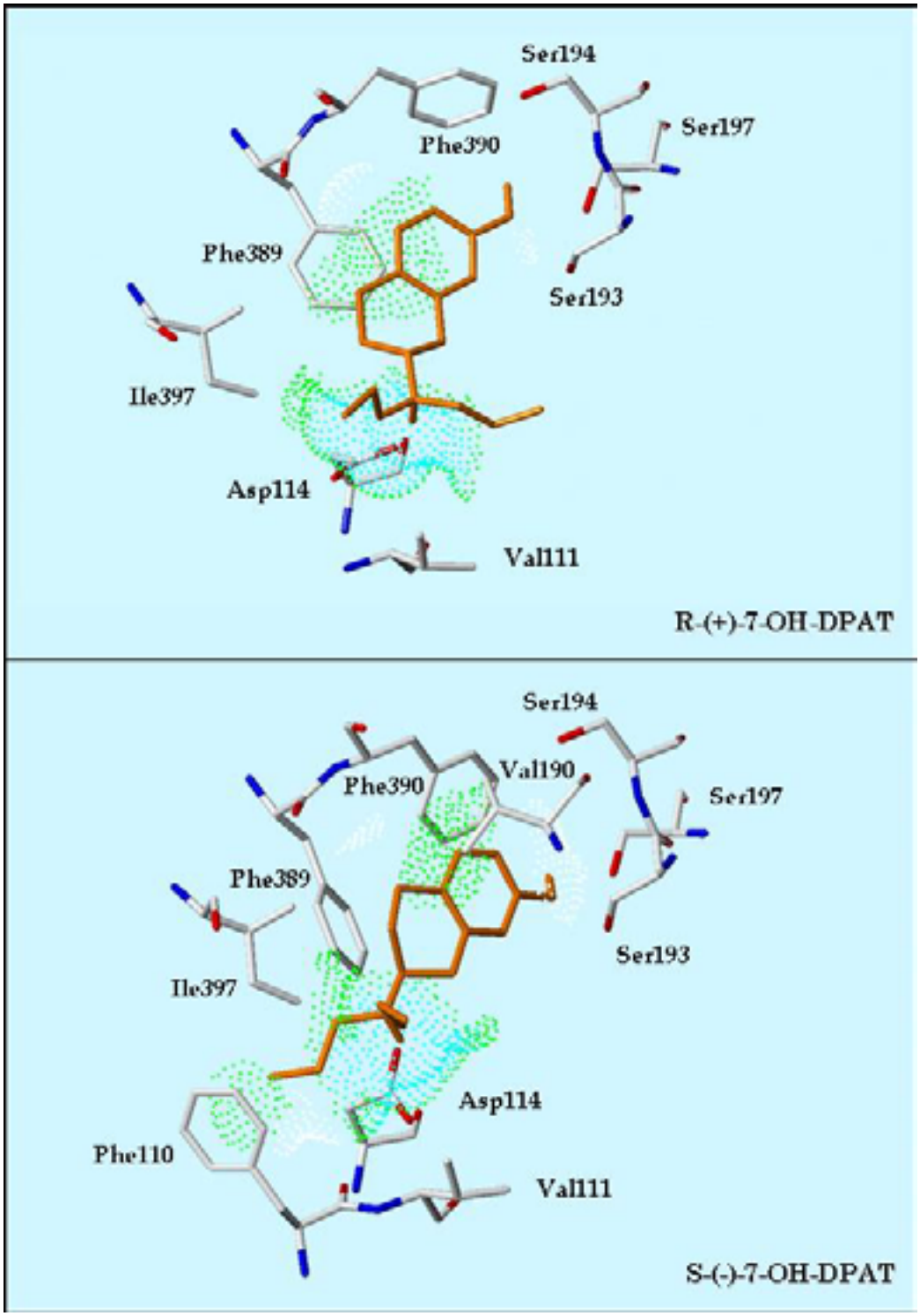

Figure 2. Binding modes for (R)–(+)–and (S)–(–)–7–OH–DPAT. Scores (similarity between the intrinsic and perceived MLP of ligands in their bound conformations) are displayed on the molecular surface S+ generated with the standard software SYBYL using the atomic radii of Gavezzotti enhanced by 0.3 Å. The color coding for the score function follows a scale starting from the most dissimilar regions to the most similar regions with the following colors: red, yellow, white, green, green–blue, blue.

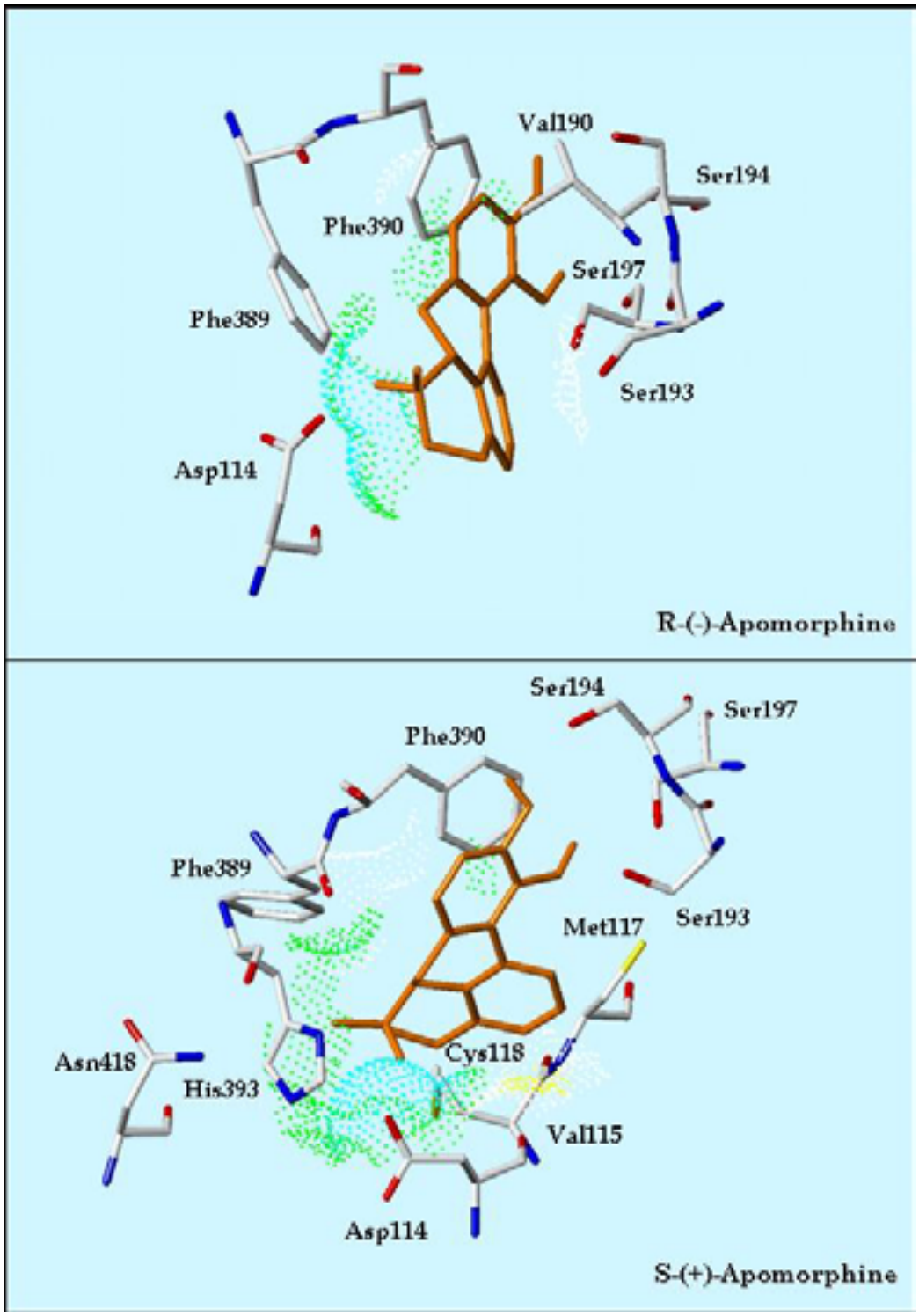

Figure 3. Views of binding mode and score function of (R)–(–)– and (S)–(+)–apomorphine in their bound conformations. For color coding, see Figure 2.

3.3 Bromocriptine

For this ligand, whose size is twice that of the other D_2 agonists in the set, the binding mode used in the cases of the other compounds was initially explored (bromocriptine1). Even if stable complexes were obtained, the similarity score displayed large regions of unfavorable interactions

(see Table 2, graphical results not shown).

Other binding modes were therefore investigated. The best solution (bromocriptine2) was retained, showing bromocriptine to form an ionic bond between its protonated amino group and Asp114 (Figure 4), with the rest of the molecule located between helices V and VI. Highly favorable ligand–receptor interactions are revealed by the MLP similarity score between the ligand and Asp114, Val115, Ser193, Ser194 and Phe390. Around the bromo atom, Met116, Pro423 and Thr427 form a binding pocket located between helices III and VII. A remarkable feature seen in the complex is the coiling of bromocriptine around TM VI. This helix is believed to be the most mobile part of the receptor because a large extracellular loop is attached to it, allowing it to accommodate large ligands such as bromocriptine.

It is of interest to note that the MLP is the only tool able to demonstrate in a straightforward manner the existence of such a hydrophobic pocket. This of course is due to the fact that hydrophobicity is encoded in lipophilicity. To obtain the same information with a force field, water should be explicitly taken into account. However, some unfavorable interactions remain in this complex; they involve Phe390 and Ile394, as revealed by the yellow and white zones in the MLP similarity score. Modeling experiments showed that the hydroxyl group may form an H–bond with Ser194.

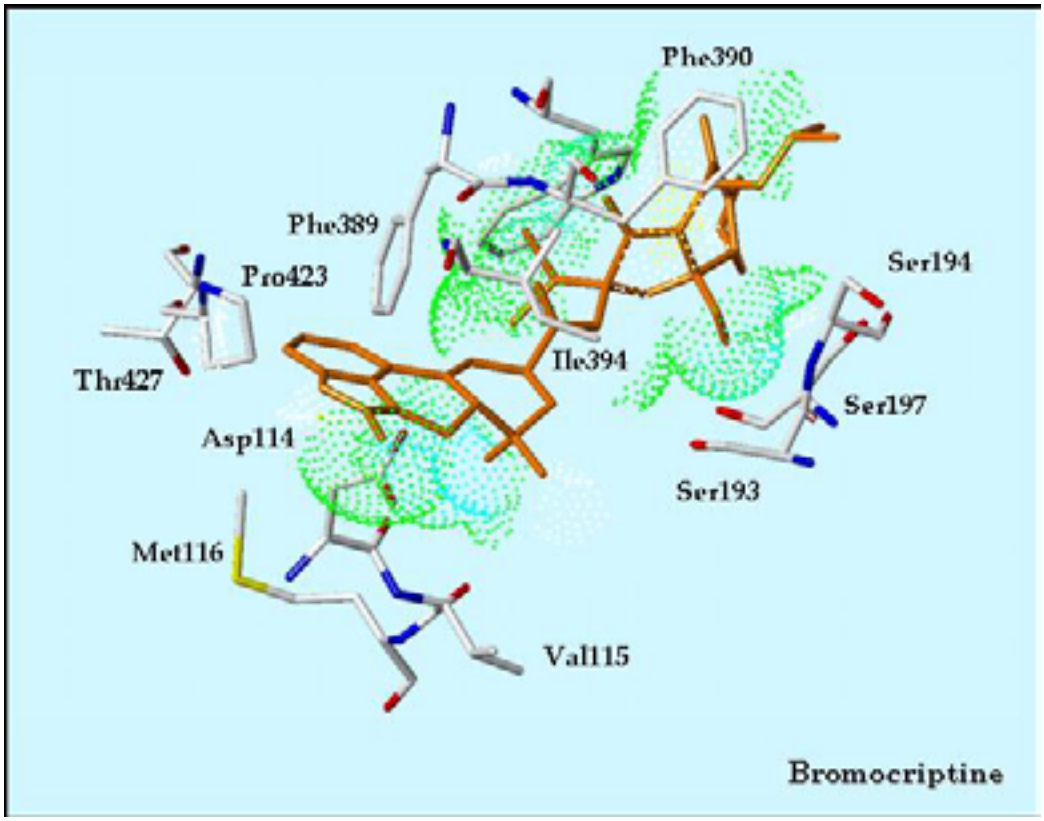

Figure 4. Views of binding mode and score function of bromocriptine in its bound conformation. For color coding, see Figure 2.

3.4 (R)–(–)–Propylnorapomorphine

Figure 5 shows that (R)–(–)–propylnorapomorphine (NPA) binds similarly to (R)–apomorphine, and indeed the MLP similarity score indicates interactions in the same regions. The structural difference between NPA and (R)–apomorphine is the size of the amino group, resulting in an additional and favorable hydrophobic interaction of NPA with Val111, shown by a wider and more intense region (see the score value) of high MLP similarity. This additional interaction may explain the greater affinity of NPA compared to (R)–apomorphine, and it rationalizes the known requirement of N–di–*n*–propyl substituent on 2–aminotetralins for greater D_2 receptor affinity [36,37]. Further studies [37] show that an aromatic substituent on the aromatic, e.g. a thienyl ring, may also increase affinity. The steric hindrance of a thienyl ring is equivalent to that of an *n*–propyl group, but thienyl allows an additional strong π–π stacking interaction. This interaction may be strong due to the electron density difference between the phenyl ring of Phe110 and the thienyl ring.

Two possible H–bonds can exist between the two hydroxyl groups of NPA and Ser193 and Ser194, like for (R)–apomorphine. Hence, and as stated above, the additional interaction of an N–di–*n*–propyl substituent with Val111 may explain the greater affinity of NPA compared to (R)–apomorphine.

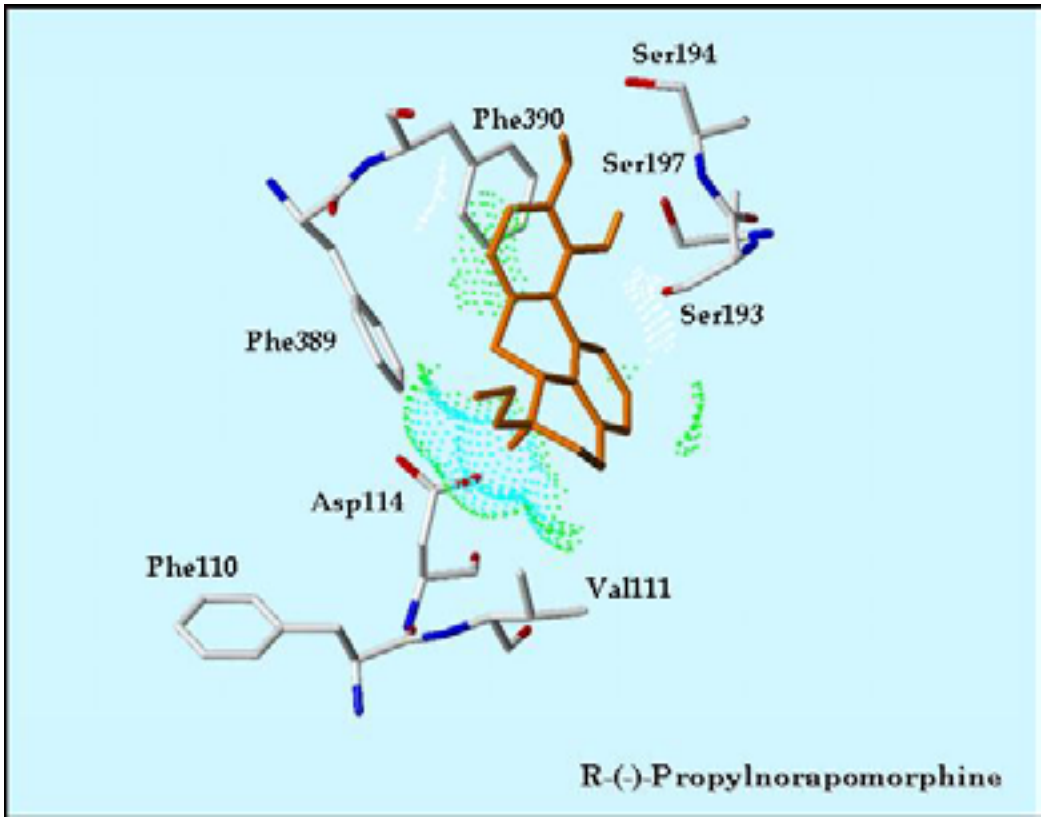

Figure 5. Views of binding mode and score function of (R)–(–)–propylnorapomorphine in its bound conformation. For color coding, see Figure 2.

3.5 (R)–(+)–8–OH–DPAT

(R)–(+)–8–OH–DPAT is seen in Figure 6 to be docked in the cavity of the D_2 receptor like (R)– and (S)–7–OH–DPAT, and to exhibit aromatic–aromatic interactions with Phe389 and Phe390. The N–alkyl group interacts positively with His393. The difference in affinity between (R)–(+)–8–OH–DPAT and the R–enantiomer of 7–OH–DPAT appears to be due to detrimental interactions of the aromatic part of the ligand with Ser193 and Ser194. The only possible H–bond found in the modeling experiments is between Ser193 and the 8–hydroxyl group.

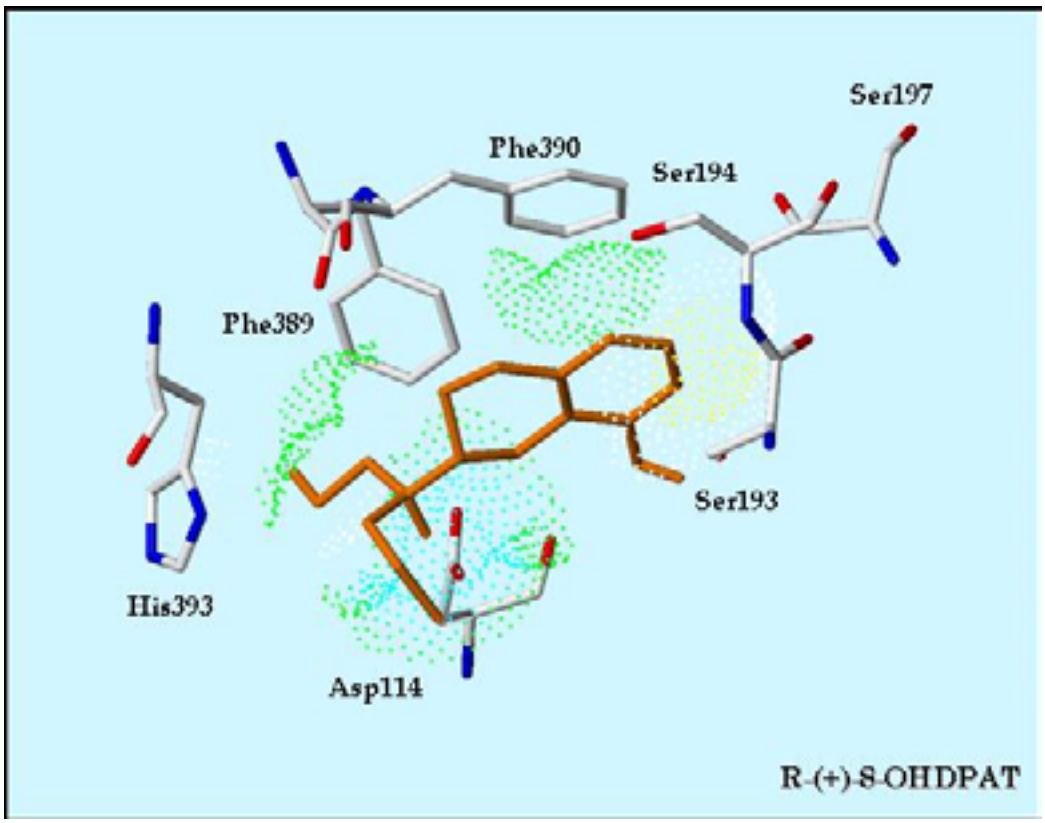

Figure 6. View of binding mode and score function of (R)–(+)–8–OH–DPAT in its bound conformation. For color coding, see Figure 2.

3.6 (R)–(+) and (S)–(–)–5–OH–DPAT

As in every complex, an extended and intense electrostatic interaction between the Asp114 side chain and the protonated amino group of the ligand is seen for (R)–(+)–5–OH–DPAT, which exhibits π–stacking interactions with Phe390. Good interactions exist also between one of the N–*n*–propyl chain of the R–enantiomer and Val111, Leu171 and Ile397. Also, an unfavorable interaction is found between His393 and the other N–*n*–propyl chain. A broad unfavorable region due to interactions of the polar Ser193 and Ser197 with the hydrophobic region of the molecule is seen.

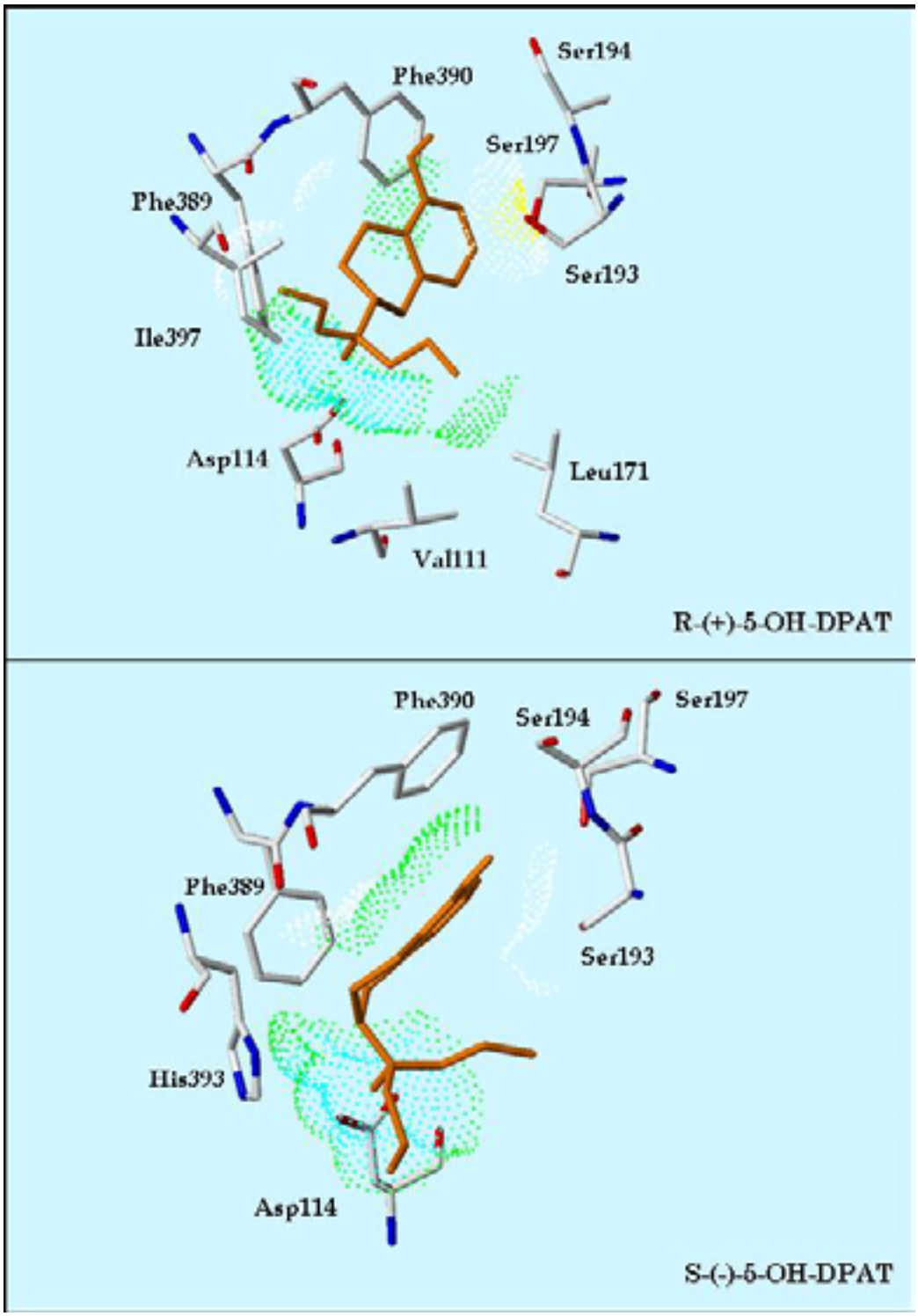

Figure 7. Views of binding mode and score function of (R)–(+)– and (S)–(–)–5–OH–DPAT in their bound conformations. For color coding, see Figure 2.

Similarly, an extended area of analogous MLPs is observed between the Asp114 and His393 side–chains and the protonated amino group of the S–enantiomer. Furthermore, a large stacking area between Phe390 and Phe389 and the aromatic part of the ligand is seen. The only two small dissimilarity areas are produced by two unfavorable interactions, namely between the Ser197 and

Ser193 and the aromatic part of the ligand, and between the peptide carbonyl linking Phe389 and Phe390 with the non–aromatic ring of the ligand. The S–enantiomer of higher affinity produced broader similarity areas and very small dissimilarity areas. As a result, the enantioselective affinity can be explained by the two different patterns.

The search for possible H–bonding indicated that no direct hydrogen bond with serine residues exists the (R)–(+)– and (S)–(–)–5–OH–DPAT. Based on molecular dynamics simulations, the hydroxyl group is too removed from the serines to allow H–bonding; however, a relay with water molecules cannot be excluded since simulations were conducted in absence of explicit water molecules.

3.7 Semi–Quantitative Interpretation

The observations with individual ligands can be summarized as follows:

An interaction between the cationic nitrogen of dopamine agonists and Asp114 was always the primary anchor point in the docking strategy and remained the stronger component of the similarity function.

1 Ser193, Ser194 and Ser197 can be involved in H–bonding with available catechol or hydroxyl groups.

2 Moreover, an aromatic stacking interaction could be seen for all ligands between their aromatic ring and Phe390 or Phe389, plus sometimes an aromatic edge–to–face interaction with Trp386.

3 Moreover, an aromatic stacking interaction could be seen for all ligands between their aromatic ring and Phe390 or Phe389, plus sometimes an aromatic edge–to–face interaction with Trp386.

Important information on modes of docking can be obtained when comparing the lipophilicity fields of a ligand and a binding site, as proposed by Eq. (3). First, on looking at the examples presented above, the MLP similarity score can be a successful novel tool for visual help in the docking procedure when no information is available on the anchor points. Second, this MLP similarity score enables us to rank the low–energy conformers of a complex, and thus becomes a criterion of selection for the best binding mode. Interestingly, the methodology presented here also allows to explain the difference in D_2 affinity between two enantiomers of a ligand and between two structurally close compounds.

A direct correlation between the MLP similarity score and the binding affinity (Table 1) was not observed. The main limitation in this approach is inherent to the numerous assumptions associated with the construction of a protein structure by homology (quality of the chosen template, neglect of loops, neglect of water molecules, *etc*.). Moreover, the current MLP similarity score appears too

simple to account quantitatively for the relative affinity of various ligands, mainly due to the fact that of lipophilicity measured in the *n*–octanol/water system encodes only part of the H–bonding capacity of solutes [38,39], namely their H–bond acceptor capacity. Thus, similarity scores based on a better description of hydrogen bonds in complexes must be proposed. A molecular hydrogen–bonding potential is currently being developed in our laboratory [40].

3.8 Comparison with Other Score Functions

To predict the binding affinity of a ligand or at least to rank some active compounds is one of the key problems in designing compounds with high affinity. Several score functions have been described [41–47]. The present score function is original in the sense that it relies on a molecular potential rather than on a set of parameters describing the free energy of binding. Some of the published score functions include lengthy calculations, others are empirical.

The latter were first developed by Böhm [48–50] and then by Eldridge *et al*. [51,52], Wang *et al*. [53] and Jain [54]. They consist in simple empirical score functions to estimate the free energy of binding for a protein–ligand complex of known 3D structure. They can be used in screening database hits (very short calculation times), or as functions to guide docking.

Some terms of the free binding energy are, however, quite hard to quantify using available approaches (*e.g*., entropic contributions). Thus, some authors [55] derived simplified potentials from known structural data to directly estimate the total protein–ligand of free energy binding, where all relevant contributions are implicitly taken into account.

In summary, the differences between existing score functions and the one presented here are:

1 A degree of similarity between the ligand and the receptor in terms of lipophilicity potential is calculated here, not an energy value.

2 Existing score functions attempt to predict the most accurate free energy of binding and not a ranking of different binding modes.

3 Existing score functions are used in screening large databases of hits (very short calculation times).

4 Most of them have no graphic interface or visual interpretation.

4 CONCLUSIONS

In the present study, a MLP similarity score is presented as a graphical tool to analyze recognition forces between a ligand and a binding site. This method allows an explanation of the difference in affinity of D_2 receptor between two enantiomers of a ligand and between two structurally related compounds. The MLP similarity score can be a successful tool for visual help in

the docking procedure. Also, this MLP similarity score has enabled us to rank the low–energy conformers of a complex, and can thus serve as a criterion of selection for the "best" binding mode.

A direct correlation between the MLP similarity score and binding affinity was, however, not observed. Clearly, quantitative correlations call for a better structural model and, perhaps, for an improved MLP and a better similarity function. Indeed, the MLP similarity score is based on information obtained from *n*–octanol/water lipophilicity and does not take π–cation interactions and H–bond donor capacities into account. Molecular lipophilicity potentials coding for the H–bond donor capacity and ionic interactions appear as a worthwhile objective.

Acknowledgment

B.T. and P.A.C. are indebted to the Swiss National Science Foundation for support. D.J.M was supported by a studentship from BBSRC.

5 REFERENCES

[1] Part of this work was presented in parts at several meetings (I. Raynaud, P. A. Carrupt, G. Caron, G. Ermondi, P. Gaillard, A. Pagliara, S. Rey, F. Billois and B. Testa, *Similarité: potentiel de lipophilie moléculaire* (*MLP*) *et potentiel de liaison hydrogène* (*MHBP*), **28 et 29 April 1998**, **Tripos User's Meeting 1998**, **Fresnes**; I. Raynaud, P.A. Carrupt, S. Rey, M. Rabii, G. Caron, G. Ermondi, A. Pagliara, P. Gaillard, B. Testa. *Additional tools for molecular modeling*, **15 July 1999**, **European Congress of Biotechnology**, **Bruxelles**; I. Raynaud, P.A. Carrupt, D.J. McLoughlin, F. Billois, P. Gaillard, P.G. Strange, B. Testa. *7–TM Receptor modeling: Use of molecular lipophilicity potentials*, **26 May 2000**, **Journées franco–belges de Pharmacochimie**, **Lille**.)

[2] N. El Tayar, B. Testa, and P. A. Carrupt. Polar intermolecular interactions encoded in partition coefficients: an indirect estimation of hydrogen–bond parameters of polyfunctional solutes. *J. Phys. Chem.* **1992**, *96*, 1455–1459.

[3] B. Testa, P. A. Carrupt, P. Gaillard, F. Billois, and P. Weber. Lipophilicity in molecular modeling. *Pharm. Res.* **1996**, *13*, 335–343.

[4] A. R. Leach. A survey of methods for searching the conformational space of small and medium–sized molecules; in: *Reviews in Computational Chemistry*, Eds. K. B. Lipkowitz and D. B. Boyd, VCH Publishers, New York, 1991, pp. 1–55.

[5] W. Heiden, G. Moeckel, and J. Brickmann. A new approach to analysis and display of local lipophilicity/hydrophilicity mapped on molecular surfaces. *J. Comput.–Aided Mol. Design* **1993**, *7*, 503–514.

[6] P. Gaillard, P.A. Carrupt, B. Testa, and A. Boudon. Molecular lipophilicity potential, a tool in 3D–QSAR. Method and applications. *J. Comput. –Aided Mol. Design* **1994**, *8*, 83–96.

[7] G.E. Kellogg, S.F. Semus, and D.J. Abraham. HINT: a new method of empirical hydrophobic field calculation for CoMFA. *J. Comput. –Aided Mol. Design* **1991**, *5*, 545–552.

[8] P. Gaillard, P.A. Carrupt, B. Testa, and P. Schambel. Binding of arylpiperazines, (aryloxy)propanolamines and tetrahydropyridyl–indoles to the 5–HT_{1A} receptor: contribution of the molecular lipophilicity potential to three–dimensional quantitative structure–activity relationship models. *J. Med. Chem.* **1996**, *39*, 126–134.

[9] S. Kneubühler, U. Thull, C. Altomare, V. Carta, P. Gaillard, P. A. Carrupt, A. Carotti, and B. Testa. Inhibition of monoamine oxidase–B by 5H–indeno[1,2–c]pyridazine derivatives: biological activities, quantitative structure–activity relationships (QSARs) and 3D–QSARs. *J. Med. Chem.* **1995**, *38*, 3874–3883.

[10] G. Folkers and A. Merz. Hydrophobic fields in quantitative structure–activity relationships; in: *Lipophilicity in Drug Action and Toxicology*, Eds. V. Pliska, B. Testa, and H. van de Waterbeemd, VCH Publishers, Weinheim, 1996, pp. 219–232.

[11] U. M. D''Souza and P. G. Strange. pH dependence of ligand binding to D_2 dopamine receptors. *Biochemistry* **1995**, *34*, 13635–13641.

[12] R. A. Williamson and P. G. Strange. Evidence for the importance of a carboxyl group in the binding of ligands to the D_2 dopamine receptor. *J. Neurochem.* **1990**, *55*, 1357–1365.

[13] B. A. Cox, R. A. Henningsen, A. Spanoyannis, R. L. Neve, and K. A. Neve. Contributions of conserved serine residues to the interactions of ligands with dopamine D_2 receptors. *J. Neurochem.* **1992**, *59*, 627–635.

[14] R. Woodward, C. Coley, S. Daniell, L. H. Naylor, and P. G. Strange. Investigation of the role of conserved serine residues in the long form of the rat D_2 dopamine receptor using site–directed mutagenesis. *J. Neurochem.* **1996**,

66, 394–402.
[15] W. Cho, L. P. Taylor, A. Mansour, and H. Akil. Hydrophobic residues of the D_2 dopamine receptor are important for binding and signal transduction. *J. Neurochem*. **1995**, *65*, 2105–2115.
[16] P. G. Strange. Dopamine receptors: studies on structure and function; in: *Advances in Drug Research*, Eds. B. Testa and U. A. Meyer, Academic Press, London, 1996, pp. 311–351.
[17] D. Donnelly, J. B. C. Findlay, and T. L. Blundell. The evolution and structure of aminergic G protein–coupled receptors. *Receptors and Channels* **1994**, *2*, 61–78.
[18] K. Palczewski, T. Kumasaka, T. Hori, C. A. Behnke, H. Motoshima, B. A. Fox, I. Le Trong, D. C. Teller, T. Okada, R. E. Stenkamp, M. Yamamoto, and M. Miyano. Crystal structure of rhodopsin: a G protein–coupled receptor. *Science* **2000**, *289*, 739–745.
[19] Tripos Associates, Inc., St–Louis, Missouri., 1995.
[20] M. Clark, R. D. Cramer III, and N. Van Opdenbosch. Validation of the general purpose Tripos 5.2 force field. *J. Comput. Chem*. **1989**, *10*, 982–1012.
[21] J. Gasteiger and M. Marsili. Iterative partial equalization of orbital electronegativity: a rapid access to atomic charges. *Tetrahedron* **1980**, *36*, 3219–3222.
[22] O. K. Baskurt, A. Temiz, and H. J. Meiselman. Effect of superoxide anions on red blood cell rheologic properties. *Free Rad. Biol. Med*. **1998**, *24*, 102–110.
[23] W. H. Press, B. P. Flannery, and W. T. Teukoslsky. Simplex; in: *Numerical Recipes in C*, *The Art of Scientific Computing*, Cambridge University Press, Cambridge, 1988, pp. 312–327.
[24] S. D. O'Connor, P. E. Smith, F. Al–Obeidi, and B. M. Pettitt. Quenched molecular dynamics simulations of tuftsin and proposed cyclic analogues. *J. Med. Chem*. **1992**, *35*, 2870–2881.
[25] M. M. Teeter, M. Froimowitz, B. Stec, and C. J. DuRand. Homology modeling of the dopamine D_2 receptor and its testing by docking of agonists and tricyclic antagonists. *J. Med. Chem*. **1994**, *37*, 2874–2888.
[26] H. G. Dohlman, J. Thorner, M. G. Caron, and R. J. Lefkowitz. Model systems for the study of seven–transmembrane–segment receptors. *Ann. Rev. Biochem*. **1991**, *60*, 653–688.
[27] C. D. Strader, M. R. Candelore, W. S. Hill, R. A. F. Dixon, and I. S. Sigal. A single amino acid substitution in the β –adrenergic receptor promotes partial agonist activity from antagonists. *J. Biol. Chem*. **1989**, *264*, 16470–16477.
[28] C. D. Strader, I. S. Sigal, R. B. Register, M. R. Candelore, E. Rands, and R. A. F. Dixon. Identification of residues required for ligand binding to the β–adrenergic receptor. *Proc. Natl. Acad. Sci. USA* **1987**, *84*, 4384–4388.
[29] C. D. Strader, I. S. Sigal, A. D. Blake, A. H. Cheung, R. B. Register, E. Rands, B. A. Zemcik, M. R. Candelore, and R. A. F. Dixon. The carboxyl terminus of the hamster β–adrenergic receptor expressed in mouse L cells Is not required for receptor sequestration. *Cell* **1987**, *49*, 855–863.
[30] P. R. Andrews and M. Tintelnot. Intermolecular forces and molecular binding; in: *Comprehensive Medicinal Chemistry*. *The Rational Design*, *Mechanistic Study & Therapeutic Applications of Chemical Compounds*, Eds. C. A. Ramsden, C. Hansch, P. G. Sammer, and J. B. Taylor, Pergamon, Oxford, 1990, pp. 321–347.
[31] D. S. Goodsell and A. J. Olson. Automated docking of substrates to proteins by simulated annealing. *Proteins: Struct. Funct. Genet*. **1990**, *8*, 195–202.
[32] P. Broto, G. Moreau, and C. Vandycke. Molecular structures: perception, autocorrelation descriptor and SAR studies. System of atomic contributions for the calculation of the n–octanol/water coefficients. *Eur. J. Med. Chem*. **1984**, *19*, 71–78.
[33] A. Gavezzotti. The calculation of molecular volumes and the use of volume analysis in the investigation of structured media and of solid–state organic reactivity. *J. Am. Chem. Soc*. **1983**, *105*, 5220–5225.
[34] P. A. Carrupt, P. Gaillard, F. Billois, P. Weber, B. Testa, C. Meyer, and S. Pérez. The molecular lipophilicity potential (MLP): a new tool for log P calculations and docking, and in comparative molecular field analysis (CoMFA); in: *Lipophilicity in Drug Action and Toxicology*, Eds. V. Pliska, B. Testa, and H. van de Waterbeemd, VCH Publishers, Weinheim, 1996, pp. 195–217.
[35] B. Testa, P. A. Carrupt, P. Gaillard, and R. S. Tsai. Intramolecular interactions encoded in lipophilicity: their nature and significance; in: *Lipophilicity in Drug Action and Toxicology*, Eds. V. Pliska, B. Testa, and H. van de Waterbeemd, VCH Publishers, Weinheim, 1996, pp. 49–71.
[36] M. P. Seiler, J. J. Bölsterli, P. Floersheim, A. Hagenbach, R. Markstein, P. Pfäffli, A. Widmer, and H. Wüthrich. Recognition at dopamine receptor subtypes; in: *Perspectives in Medicinal Chemistry*, Eds. B. Testa, E. Kyburz, W. Fuhrer, and R. Giger, Verlag Helvetica Chimica Acta, Basel, 1993, pp. 221–257.
[37] A. Malmberg, G. Nordvall, A. M. Johansson, N. Mohell, and U. Hacksell. Molecular basis for the binding of 2–aminotetralins to human dopamine D_{2A} and D_3 receptors. *Mol. Pharmacol*. **1994**, *46*, 299–312.
[38] N. El Tayar, R.S. Tsai, B. Testa, P.A. Carrupt, and A. Leo. Partitioning of solutes in different solvent systems: the contribution of hydrogen–bonding capacity and polarity. *J. Pharm. Sci*. **1991**, *80*, 590–598.
[39] M. H. Abraham, H. S. Chadha, G. S. Whiting, and R. C. Mitchell. Hydrogen bonding. 32. An analysis of water–octanol and water–alkane partitioning and the δlog P parameter of Seiler. *J. Pharm. Sci*. **1994**, *83*, 1085–1100.

[40] S. Rey, G. Caron, G. Ermondi, P. Gaillard, A. Pagliara, P. A. Carrupt, and B. Testa. Development of molecular hydrogen bonding potentials (MHBPs) and their application to structure permeation relations. *J. Mol. Graphics Model*. **2001**, *19*, 521–535.
[41] Ajay and M. A. Murcko. Computational methods to predict binding free energy in ligand–receptor complexes. *J. Med. Chem*. **1995**, *38*, 4953–4967.
[42] J. R. H. Tame. Scoring functions: a view from the bench. *J. Comput.–Aided Mol. Design* **1999**, *13*, 99–108.
[43] C. Pérez and A. R. Ortiz. Evaluation of docking function for protein–ligand docking. *J. Med. Chem*. **2001**, *44*, 3768–3785.
[44] R. D. Taylor, P. J. Kewsbury, and J. W. Essex. A review of protein–small molecule docking methods. *J. Comput.–Aided Mol. Design* **2002**, *16*, 151–166.
[45] N. Brooijmans and I. D. Kuntz. Molecular recognition and docking algorithms. *Annu. Rev. Biophys. Biomol. Struct*. **2003**, *32*, 335–373.
[46] R. Wang, Y. Lu, and S. Wang. Comparative evaluation of 11 scoring functions for molecular docking. *J. Med. Chem*. **2003**, *46*, 2287–2303.
[47] I. Halperin, B. Ma, H. Wolfson, and R. Nussinov. Principles of docking: an overview of search algorithms and a guide to scoring functions. *Proteins: Struct. Funct. Genet*. **2002**, *47*, 409–443
[48] H. J. Böhm. LUDI: rule–based automatic design of new substituents for enzyme inhibitor leads. *J. Comput.–Aided Mol. Design* **1992**, *6*, 593–606.
[49] H. J. Böhm. The development of a simple empirical scoring function to estimate the binding constant for a protein–ligand complex of known three–dimensional structure. *J. Comput.–Aided Mol. Design* **1994**, *8*, 243–256.
[50] H. J. Böhm. Prediction of binding constants of protein ligands: a fast method for the prioritization of hits obtained from de novo design or 3D database search programs. *J. Comput.–Aided Mol. Design* **1998**, *12*, 309–323.
[51] M. D. Eldridge, C. J. Murray, T. R. Auton, G. V. Paolini, and R. P. Mee. Empirical scoring functions. I. The development of a fast empirical scoring function to estimate the binding affinity of ligand in receptor complexes. *J. Comput. –Aided Mol. Design* **1997**, *11*, 425–445.
[52] C. W. Murray, T. R. Auton, and M. D. Eldridge. Empirical scoring functions. II. The testing of an empirical scoring function for the prediction of ligand–receptor binding affinities and the use of Bayesian regression to improve the quality of the model. *J. Comput.–Aided Mol. Design* **1998**, *12*, 503–519.
[53] R. Wang, L. Liu, L. Lai, and Y. Tang. SCORE: a new empirical method for estimating the binding affinity of a protein–ligand complex. *J. Mol. Model*. **1998**, *4*, 379–394.
[54] A. N. Jain. Scoring noncovalent protein–ligand interactions: a continuous differentiable function to compute binding affinities. *J. Comput. –Aided Mol. Design* **1996**, *10*, 427–440.
[55] I. Muegge and Y. C. Martin. A general and fast scoring function for protein–ligand interactions: a simplified potential approach. *J. Med. Chem*. **1999**, *42*, 791–804.
[56] B. Gardner and P. G. Strange. Agonist action at D_2(long) dopamine receptors: ligand binding and functional assays. *Brit. J. Pharmacol*. **1998**, *124*, 978–984.
[57] C. Jeandenans, P. A. Carrupt, B. Testa, and A. Michel. DISCO and CoMFA studies of D_2–type dopaminergic ligands. 11th European Symposium on QSAR: Computer–Assisted Lead Finding and optimization. *Congress* **1996**, *Lausanne*, *Sept. 1–6*, *1996*, *Abstract*, P–7.D.